

## Head-Turned Postures Increase the Risk of Cervical Facet Capsule Injury During Whiplash

Gunter P. Siegmund, PhD,\*† Martin B. Davis, MS,‡ Kyle P. Quinn, BS,§ Elizabeth Hines,§ Barry S. Myers, PhD,¶|| Susumu Ejima, PhD,|| Kishiri Ono, PhD,|| Koichi Kamiji, BS,\*\* Tsuyoshi Yasuki, MS,\*\* and Beth A. Winkelstein, PhD‡§

**Study Design.** *In vitro* experiments using cadaveric cervical spine motion segments to quantify facet capsular ligament strain during whiplash-like loading.

**Objective.** To quantify facet capsule strains during whiplash-like loading with an axial intervertebral prerotation simulating an initial head-turned posture and to then compare these strains to previously-published strains for partial failure and gross failure of the facet capsule for these specimens.

**Summary of Background Data.** Clinical data have shown that a head-turned posture at impact increases the severity and duration of whiplash-related symptoms.

**Methods.** Thirteen motion segments were used from 7 women donors ( $50 \pm 10$  years). Axial pretorques ( $\pm 1.5$  Nm), axial compressive preloads (45, 197, and 325 N), and quasi-static shear loads (posteriorly-directed horizontal forces from 0 to 135 N) were applied to the superior vertebral body to simulate whiplash kinematics with the head turned. Three-dimensional displacements of markers placed on the right facet capsular ligament were used to estimate the strain field in the ligament during loading. The effects of pretorque direction, compression, and posterior shear on motion segment motion and maximum principal strain in the capsule were examined using repeated-measures analyses of variance.

**Results.** Axial pretorque affected peak capsule strains more than axial compression or posterior shear. Peak strains reached  $34\% \pm 18\%$  and were higher for pretorques toward rather than away from the facet capsule (*i.e.*, head rotation to the right caused higher strain in the right facet capsule).

**Conclusion.** Compared to previously-reported data for these specimens, peak capsule strains with a pretorque were double those without a pretorque ( $17\% \pm 6\%$ ) and not significantly different from those at partial failure of the ligament ( $35\% \pm 21\%$ ). Thus a head-turned posture increases facet capsular ligament strain compared to a neutral head posture—a finding consistent with the greater symptom severity and duration observed in whiplash patients who have their head turned at impact.

**Key words:** neck, whiplash injury, tissue strain, coupled motion, zygapophysial joint, axial rotation. **Spine 2008;33:1643–1649**

Injury to the cervical facet capsular ligaments is a potential mechanism for chronic pain after acute whiplash injury. Distending the facet capsule by injecting contrast media has produced whiplash-like pain patterns in normal individuals,<sup>1</sup> and anesthetic blocks have isolated the cervical facet joints as the source of pain in about half of a chronic whiplash population.<sup>2</sup> More recently, *in vivo* animal models of facet capsule loading have shown that group III and IV afferents (thought to mediate pain) from the facet capsule have a graded electrical response to mechanical loading of the facet joint in the goat<sup>3</sup> and have suggested that a capsular ligament strain-threshold exists above which allodynia—pain in response to a normally nonnoxious stimulus—is produced.<sup>4</sup> These data support a facet capsule-based mechanism for whiplash injury, but do not establish whether human capsular ligaments are injured in the low-speed rear-end collisions to which many whiplash injuries are attributed.

Whiplash patients who had their head turned at impact have more severe and persistent symptoms than patients who were facing forward.<sup>5,6</sup> These findings have prompted biomechanical studies using human cadaveric necks to investigate why a head-turned posture increases injury potential. Dynamic rear-impact tests of prerotated ligamentous spines (occiput-T1) produce increased neck flexibility (interpreted as injury) in extension, lateral bending and axial rotation.<sup>7</sup> Though concentrated in the lower cervical spine, these “injuries” were not isolated to particular spinal ligaments. Detailed measurements of the strain field in the facet capsule have also shown that a head-turned posture generates higher capsular strains than a neutral head posture,<sup>8</sup> but the quasi-static loads applied during those tests were limited to pure flexion/extension moments and did not include the axial compression or posterior shear present during whiplash loading. Thus the question of how a head-turned posture

From the \*MEA Forensic Engineers & Scientists, Richmond; †School of Human Kinetics, University of British Columbia, Vancouver, BC, Canada; Departments of ‡Neurosurgery; §Bioengineering, University of Pennsylvania, Philadelphia, PA; ¶Department of Biomedical Engineering, Duke University, Durham, NC; ||Japan Automobile Research Institute, Tsukuba, Ibaraki; and \*\*Japan Automobile Manufacturers Association, Tokyo, Japan.

Acknowledgment date: August 21, 2007. Revision date: January 2, 2008. Acceptance date: February 4, 2008.

Supported by Japan Automobile Research Institute, US Department of Health and Human Services, Centers for Disease Control Grant R49/CCR402396–12, Catharine Sharpe Foundation, an International Society of Biomechanics Student Travel Grant, the Natural Science and Engineering Research Council, and the Science Council of British Columbia.

The manuscript submitted does not contain information about medical device(s)/drug(s).

Corporate/Industry, Federal and Professional Organizational funds were received in support of this work. One or more of the author(s) has/have received or will receive benefits for personal use from a commercial party related directly or indirectly to the subject of this manuscript: e.g., honoraria, gifts, consultancies, royalties, stocks, stock options, decision making position.

Address correspondence and reprint requests to Dr. Gunter P. Siegmund, MEA Forensic Engineers & Scientists, 11-11151 Horseshoe Way, Richmond, BC, Canada, V7A 4S5; E-mail: gunter.siegmund@meaforensic.com

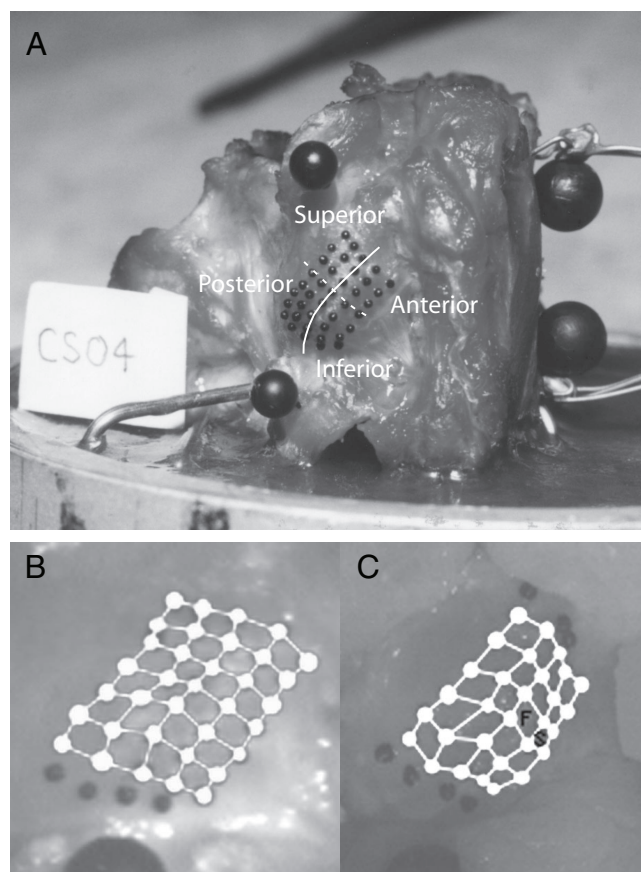


Figure 1. Sample test specimen (A) and meshed capsule arrays of the same specimen for its whiplash-like loading test (B) and failure test (C). Panel (A) also shows the 4 quadrants of the capsule used for the strain analysis. The solid white line lies along the estimated joint plane and the dashed white line intersects it perpendicularly about midway along the visible joint line. The elements with the maximum principal strain at failure (F) and partial failure (S) are each shown in panel (C).

combined with multiaxial whiplash loads affects facet capsular ligament strain has yet to be answered.

Our goals were to use human cadaveric motion segments to: (1) quantify the intervertebral kinematics and facet capsule strains under whiplash-like loads in the presence of an initial axial rotation, and (2) compare the capsule strains generated by these combined loads to the previously-published strains needed to injure these ligaments in isolated shear failure.<sup>9</sup> Our overall hypothesis was that capsular strains during this simulated whiplash exposure are similar to those needed to injure the capsular ligament.

## Methods

### Specimen Preparation

Thirteen motion segments (7 C3/4; 6 C5/6) from 7 unembalmed female human cadavers ( $50 \pm 10$  years; mean  $\pm$  SD) were isolated for mechanical testing. Vertebral bodies were cast with the mid-discal plane horizontal using polyester resin and stainless steel wires (Figure 1). Multiple black spheres were attached to the specimen for motion analysis: 4 markers (7.94 mm diameter) to each vertebral body to quantify vertebral motion, 2 markers (4.76 mm) to the right articular processes su-

perior and inferior to the capsular ligament, and an array of markers (0.79 mm) to the lateral aspect of the right capsular ligament (Figures 1, 2). Ligament marker arrays varied from  $5 \times 7$  markers to  $7 \times 7$  markers and covered an area of about  $1 \text{ cm}^2$ .

### Test Equipment

The inferior vertebra was cast in a cup rigidly attached to the test frame through a 6-axis load cell (Denton 1716A, R.A. Denton, Farmington Hills, MI) (Figure 2). Axial compression was applied statically using weights placed in a cradle attached to the superior casting cup.<sup>9</sup> Axial pretorques were applied as a force couple to the superior casting cup and posterior shear loads were applied through a yoke also attached to the superior casting cup (Figure 2).<sup>8,9</sup> Two  $119 \times 192$  pixel cameras (EktaPro, Eastman Kodak, Charlotte, NC) recorded the vertebral markers and two  $640 \times 480$  pixel cameras (Pulnix TN-9701, Pulnix America Inc., Sunnyvale, CA) recorded the capsule marker arrays. The system-wide root mean square errors for determining marker positions were  $<0.18 \text{ mm}$  in translation and  $<0.73^\circ$  in rotation for vertebral markers, and  $<0.06 \text{ mm}$  for capsule markers.

### Test Procedures

Each specimen was preconditioned by 30 flexion/extension cycles before undergoing step-wise posterior shear loading (0–135 N in 11 steps) under 10 different combinations of axial compression (0, 45, 197, and 325 N) and axial pretorque (0 and  $\pm 1.5 \text{ Nm}$ ) (Table 1). Because the right facet joint was studied here, a pretorque to the right (+z) is an ipsilateral pretorque and a pretorque to the left (–z) is a contralateral pretorque. The line of action of the shear force was 8.5 mm above the mid-discal plane and therefore produced an extension moment across the intervertebral joint. Specimens were allowed to creep for 30 seconds at each shear step before load cell and image data were simultaneously acquired. Data from the 6 preload conditions that combine axial compression and axial pretorque (numbered 5 through 10 in Table 1) are reported here; data from the 4 compression-only preload conditions were reported previously.<sup>9</sup>

The shear loads were based on peak horizontal shear forces between 40 and 250 N at the atlanto-occipital joint in human subjects during an 8-km/h rear-end impact.<sup>10,11</sup> Compressive loads represented head weight (45 N),<sup>12</sup> the combination of head weight and inertial neck compression developed by torso-seatback interaction (197 N),<sup>10,13</sup> and the combination of head weight, inertial compression and reflexive muscle forces (325 N).<sup>14</sup> Axial pretorques were based on previous work showing that 1.5 Nm at these vertebral levels produces  $1.9 \pm 1.0^\circ$  of rotation,<sup>8</sup> slightly less than the  $3.0$  to  $4.5^\circ$  range reported *in vivo* at maximal head rotation.<sup>15,16</sup>

### Data Reduction

Three-dimensional coordinates of the vertebral and capsule markers were computed from the digitized stereo-image pairs using direct linear transformation.<sup>17,18</sup> All marker displacements were referenced to the same initial configuration, which corresponded to 45 N of axial compression with no posterior shear or axial pretorque (condition 2, Table 1). This reference configuration represents a relaxed, forward-facing occupant before a rear-end collision. Angular displacements of the vertebra are reported as Cardan-Bryant angles decomposed as flexion/extension first, then axial rotation, and then lateral flexion. Movement of 1 or more of the 4 vertebral markers after

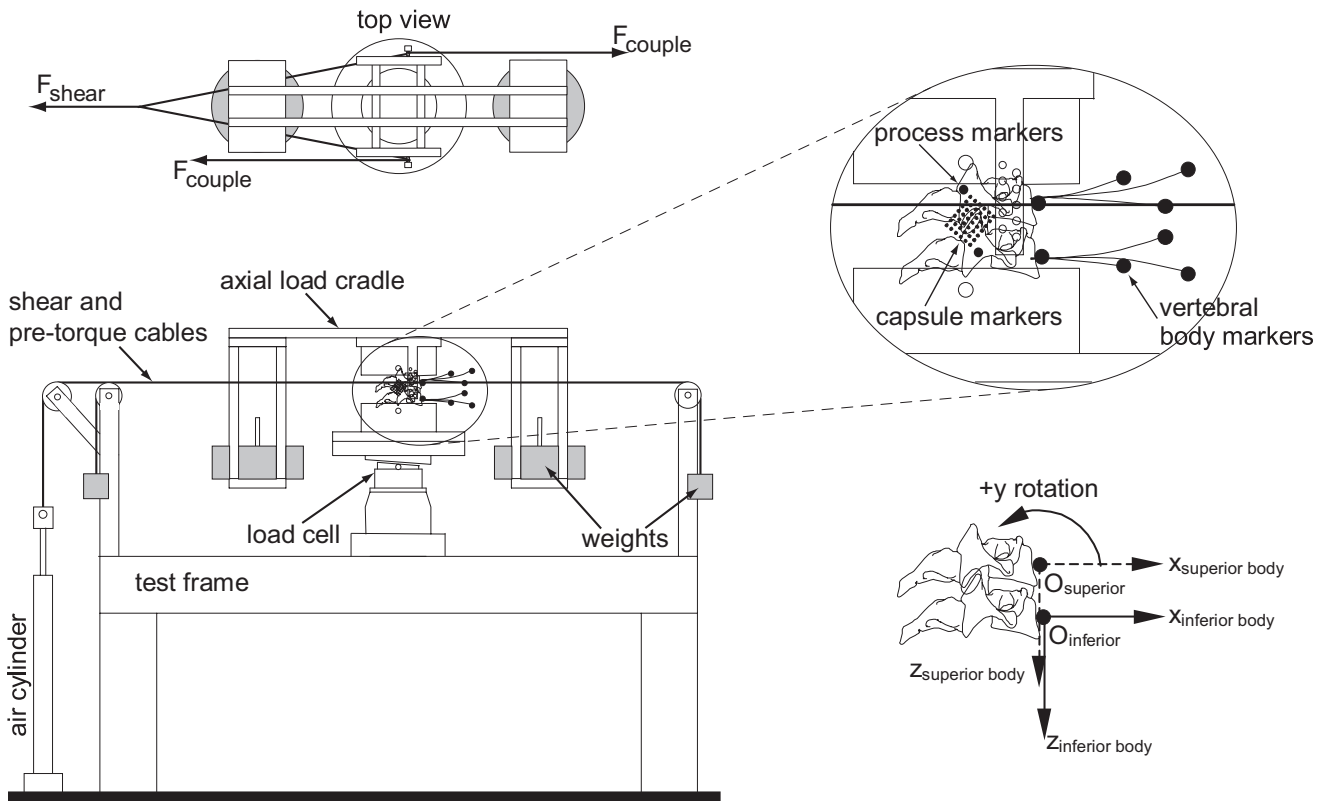


Figure 2. Schematic of the test setup, motion analysis markers and reference frames. The force couple ( $F_{couple}$ ) shown in the top view produces an ipsilateral pretorque ( $+M_z$ ); the reverse couple produces a contralateral pretorque ( $=M_z$ ).

the 45 N neutral test condition eliminated 4 specimens (3 at C3/4 and 1 at C5/6) from the vertebral motion data set. Applied loads are reported relative to the stationary reference frame of the inferior vertebra (Figure 1).

The three-dimensional coordinates of the capsule markers were used to create a mesh of 4-node shell elements. Capsule motion over the curved joint surface obscured some markers and prevented every marker from being used in the mesh. As a result, mesh sizes varied from  $4 \times 4$  markers to  $6 \times 6$  markers or  $5 \times 7$  markers (Figure 1B,C). A customized isoparametric mapping program (Matlab 7.2; Mathworks Inc., Natick, MA) was used to compute the deformation gradients, corresponding planar strains, and principal strain fields from the three-dimensional displacements of the capsule markers at each applied load. The maximum principal strain (MPS) across all analyzed elements was then determined at each shear step for each combined preload condition.

**Comparison to Failure Data**

For the second part of this study, the capsule strains in the combined loading configurations were compared to the strains

at partial failure and gross failure reported previously for these specimens.<sup>9</sup> Because some capsule markers were lost during isolation of the facet joint for failure testing and other markers were obscured from one camera’s view by intervertebral rotation in the current data set, an element-by-element comparison of combined-loading strains and failure strains was not possible. Therefore, each ligament was divided into 4 quadrants (superior, anterior, inferior, posterior) based on the joint anatomy (Figure 1A) and the MPS was determined for the elements within each quadrant at each shear step for each combined preload condition. For comparison, the previously-published strain data from the failure tests were reanalyzed to define the MPS according to these same quadrant regions.

**Statistical Analysis**

The effects of the combined loading on both intervertebral motion and MPS in the capsule were analyzed. For intervertebral motion, the effects of axial compression (45, 197, 325 N), posterior shear (0–135 N in 11 steps), and axial pretorque (+1.5 Nm, –1.5 Nm) on each of the 6 of vertebral motion directions (3 translations:  $T_x, T_y, T_z$ ; and 3 rotations  $R_x, R_y, R_z$ ; Figure 2) were tested using a 3-way, repeated-measures analysis of variance. For MPS in the capsule, the effects of these same 3 independent variables and capsule quadrant (superior, anterior, inferior, posterior) were tested using a 4-way, repeated-measures analysis of variance. The magnitudes of MPS in the combined-loading, partial failure, and gross failure conditions were compared using paired *t* tests. The distribution of MPS across the 4 quadrants was examined by first counting the number of specimens for which MPS occurred in each quadrant, and then comparing these counts using pair-wise binomial tests. All statistical tests were performed using Statistica (v.6.1, Statsoft Inc., Tulsa, OK) at a significance level of  $\alpha = 0.05$ .

**Table 1. Test Order of the Preload Conditions for All Specimens**

Axial Preload	Axial Pretorque		
	None	+1.5 Nm (Ipsilateral)	–1.5 Nm (Contralateral)
0 N	1	—	—
45 N	2	5	6
197 N	3	8	7
325 N	4	9	10

Dash indicates cells not tested.

**Table 2. P-Values of the Significant Effects for the Three-Way ANOVA Used for Vertebral Motion ( $T_x$  Through  $R_z$ ) and for the Four-Way ANOVA Used for Maximum Principal Strain (MPS) in the Facet Capsule**

Dependent Variable	Statistical Analysis (P)					
	Main Effects			Interactions		
	Quadrant	Compression	Torque	Shear	C × S	T × S
$T_x$	—			0.0003		
$T_y$	—		0.043			
$T_z$	—					
$R_x$	—		0.025			
$R_y$	—	0.0005		<0.0001		
$R_z$	—		0.0002			0.002
MPS	0.023		0.020		<0.0001	0.0005

Interactions not shown were not significant. Interactions expressed using the first letter of the main effect.

**Results**

In response to the multiaxial loads applied to the motion segment, the superior vertebra translated posteriorly, extended, and rotated axially in the direction of the applied pretorque (*P*-values given in Table 2, Figure 3). In addition to these primary motions, coupled motions in lateral translation, and lateral flexion were also observed (Figures 3B, D). Despite a constant axial pretorque, the axial rotations established by the initial pretorques (Figure 3F) diminished as the shear load increased and

were no longer significantly different at shear loads of 96 and 135 N.

MPS in the facet capsule was affected more by axial pretorque than either axial compression or posterior shear (Table 2, Figure 4). At all but the lowest shear loads, MPS was higher for the ipsilateral pretorque than the contralateral pretorque (Table 2, Figures 4A, B) and reached a maximum of  $34\% \pm 18\%$  at 96 N of shear when pooled across compressive preloads (MPS did not vary with compression, Table 2). Within-specimen differences between the ipsilateral and contralateral strains were greatest at shear loads of 50 to 100 N (Figure 4D).

MPS in the facet capsule occurred most frequently in elements located in the superior and anterior quadrants of the capsule. Across all shear steps, the magnitude of the MPS was less in the inferior quadrant than in either the anterior or superior quadrants (*post hoc*, *P* = 0.045 and 0.054 respectively; Figure 4C). For the ipsilateral pretorque, the location of MPS at zero shear occurred most frequently in the superior and anterior quadrants (Figure 5A). A similar pattern was not observed for the contralateral pretorque (Figure 5C). At maximal posterior shear, the location of the MPS occurred most frequently in the superior quadrant for the ipsilateral condition and in the anterior quadrant for the contralateral condition (Figures 5B, D). MPS at maximum posterior shear occurred least frequently in the inferior quadrant under both pretorque conditions (Figures 5A–D).

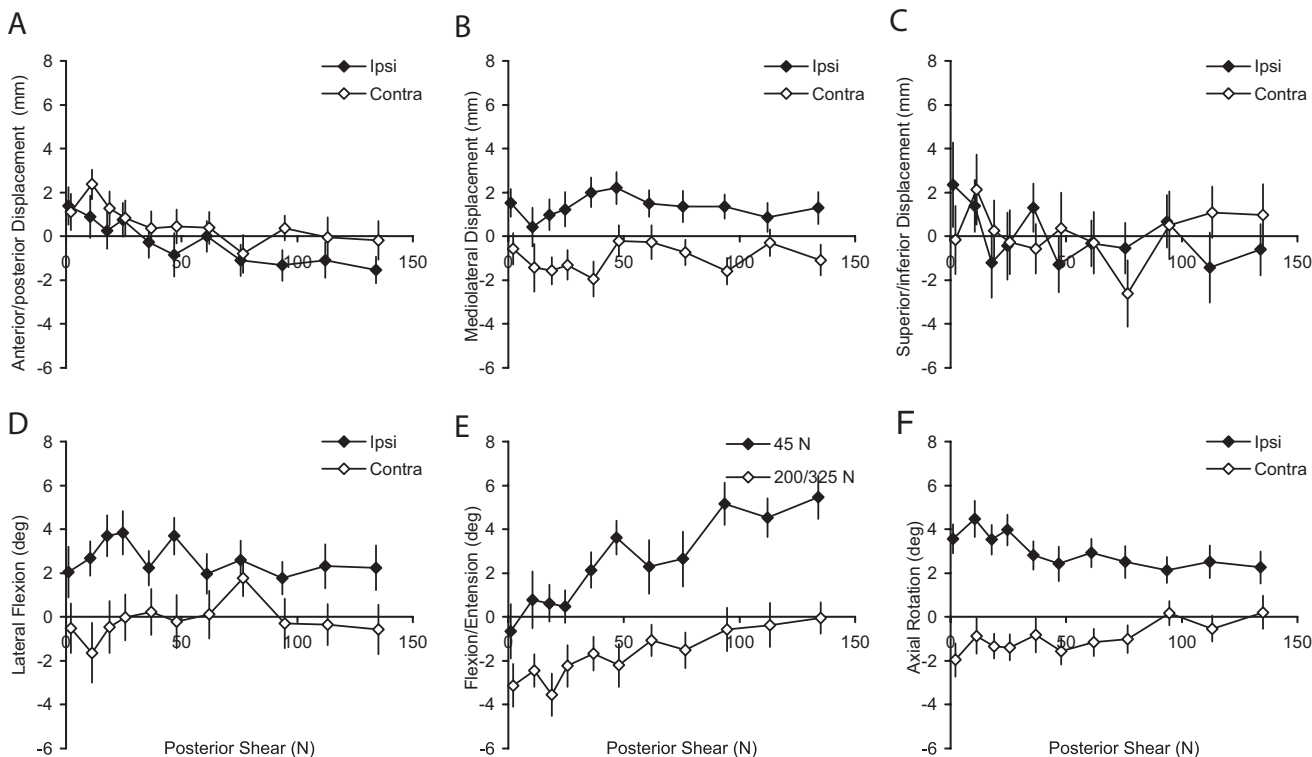


Figure 3. Summary plots of the linear (A–C) and angular (D–F) displacements of the superior vertebral body with respect to the x, y, and z axes of the inferior vertebral body. Conditions not significantly different from one other have been pooled in some of the graphs. The error bars depict standard error (SE). Ipsi, ipsilateral; contra, contralateral.



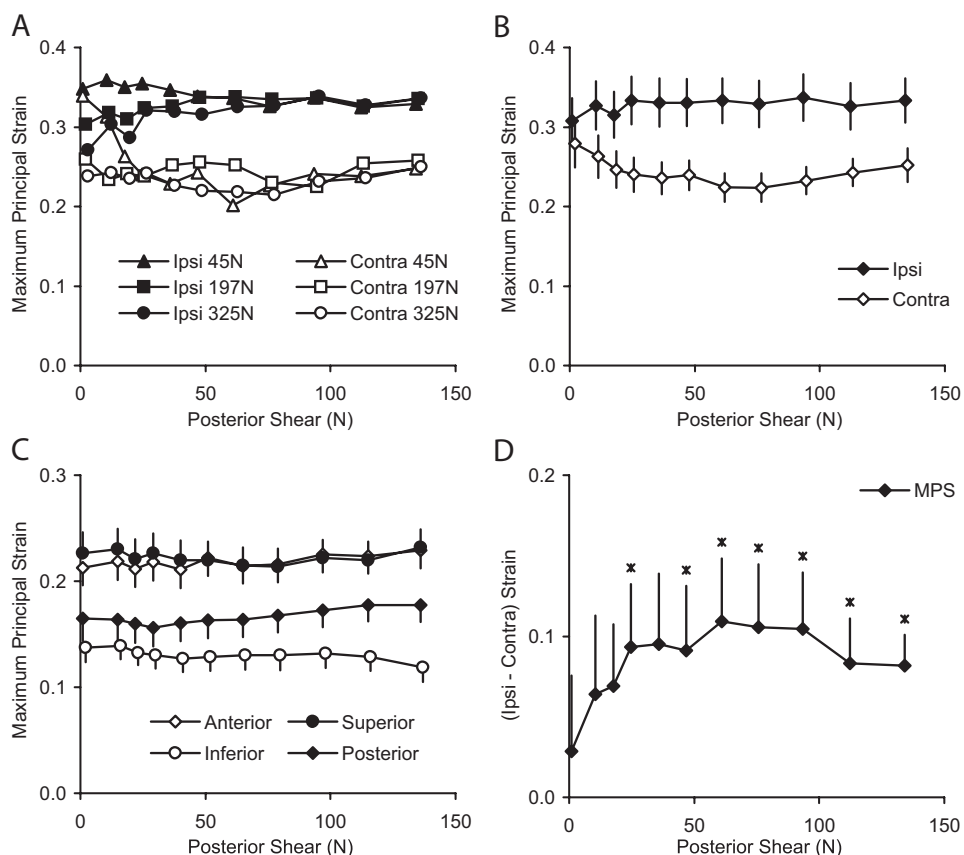


Figure 4. Summary plots of maximum principal strain (MPS) in the facet capsule as a function of applied posterior shear. MPS for each preload condition (A) and for both ipsi- and contralateral pretorque conditions pooled across axial preloads (B). Also shown are maximum principal strain within each quadrant for all axial preload and pretorque conditions pooled (C) and the within-specimen difference in MPS between the ipsi- and contralateral conditions (D). Asterisks in (D) depict differences significantly greater than zero. Error bars depict standard error (SE).

When the previously-published failure data were partitioned into the 4 quadrants defined here, MPS at gross failure (previously reported to be  $94\% \pm 85\%$ )<sup>9</sup> occurred most frequently in the superior and inferior quadrants (Figure 5F). MPS at partial failure (previously reported to be  $35\% \pm 21\%$ )<sup>9</sup> occurred most frequently in the inferior quadrant (Figure 5E). A quadrant-by-quadrant comparison revealed that peak strains produced by the multiaxial whiplash-like loads reached  $84\% \pm 51\%$  of the strains causing partial failure ( $P = 0.19$ ) and  $66\% \pm 83\%$  of the strains causing gross failure ( $P = 0.02$ ). When compared quadrant by quadrant, the MPS observed during the multiaxial tests exceeded the partial failure strain in 2 specimens and exceeded the gross failure strain in 2 other specimens.

## Discussion

Axial pretorque and the resulting axial rotation of the intervertebral joint have a large effect on the MPS in the cervical facet joint capsule when combined with compression, shear, and extension loads simulating a low-speed rear-end automobile impact. Peak strains in the capsule with an ipsilateral pretorque ( $34\% \pm 18\%$ ) were double the previously-reported peak strains without a pretorque ( $17\% \pm 6\%$ ) but similar to the previously-reported strains to cause partial failures ( $35\% \pm 21\%$ ) in these specimens.<sup>9</sup> These findings potentially explain the increased severity and persistence of whiplash symptoms in patients who had their head turned at impact.<sup>5,6</sup>

Axial pretorque alone contributes considerably to peak strain. Before applying the shear load, axial pretorque produced large strains in the capsule for both the ipsilateral (31%) and contralateral (28%) conditions (Figure 4B). Using the same pretorque magnitudes, Winkelstein *et al*<sup>8</sup> reported lower strains in the ipsilateral (12%) and contralateral conditions (22%). These differences, however, could be related to the presence of a compressive preload and the use of female rather than male specimens in the current study. Further work is needed to explore these issues.

In the ipsilateral condition, MPS initially occurred most frequently in the superior and anterior quadrants of the capsule (Figure 5A). When shear was added, MPS increased by about 3% (Figure 4B) and concentrated in the superior quadrant (Figures 5B). In the contralateral condition, however, MPS did not initially occur more frequently in a particular quadrant (Figure 5C). When shear was added to the contralateral pretorque, MPS decreased by about 6% before then increasing (Figure 4B) and concentrated in the anterior quadrant (Figure 5D). This combination of findings suggests that posterior shear and the ipsilateral pretorque strain similar parts of the capsule and thus MPS in the capsule continues to increase when shear is added. Conversely, posterior shear and the contralateral pretorque appear to strain different parts of the capsule and thus MPS in the capsule is initially relieved when shear is added (Figure 4B). Viewed more broadly, these findings suggest that the

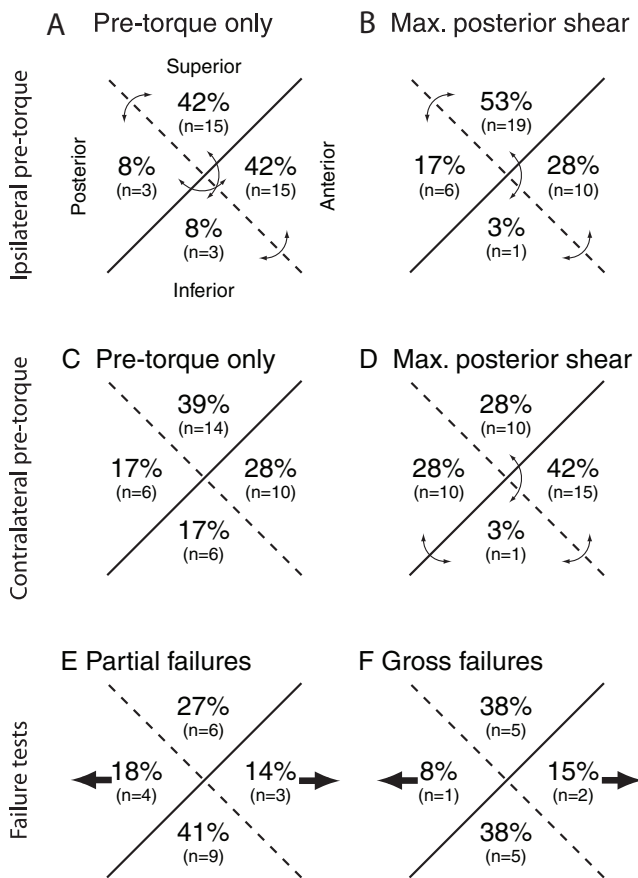


Figure 5. Distribution of the maximum principal strains within the 4 quadrants of the capsular ligament. Data from 12 specimens are shown for the whiplash-like loading tests (top 2 rows) for the ipsilateral (A, B) and contralateral (C, D) pretorque conditions with no posterior shear (A, C) and maximum posterior shear (B, D). Each axial compression level (45, 197, and 325 N) is treated as a single test (A–D). Curved arrows show significantly different proportions based on binomial comparisons ( $P < 0.05$ ). Data from the failure tests include 22 partial failures (E) observed before gross failure (F) of the 13 ligaments. Large arrows in panels E and F depict direction of loads used in the failure tests. Solid and dashed lines depict the capsule quadrants defined in Figure 1. Quadrant labels repeated in panel (A) for clarity.

facet capsules located on the side of the neck towards which a vehicle occupant’s head is turned are most likely to be injured in a rear-end crash, although we could find no clinical or epidemiological data to support or refute this proposition.

The small increase in strain when posterior shear was added to an ipsilateral pretorque was unexpected and suggests that peak capsule strain is relatively insensitive to increasing posterior shear (Figures 4A–C). This conclusion, however, may be confounded by the simultaneous reduction in intervertebral axial rotation observed with increasing posterior shear (Figure 3F). As shear increases, this unwinding of the initial axial rotation may reduce capsule strain at the same time that posterior shear increases capsule strain. As a result, our experimental set up may not capture the true contribution of posterior shear to capsule strain. If the axial rotation imposed by the pretorque had remained constant

throughout the applied posterior shear, then capsule strain would be expected to increase more steeply with posterior shear, particularly in the ipsilateral condition. Based on recent dynamic *in vivo* data,<sup>19</sup> the head’s inertia is expected to maintain or even increase intervertebral axial rotation as posterior shear develops. Thus under the dynamic conditions of actual whiplash exposures, the unwinding of an initial axial rotation observed here is unlikely to occur and the contribution of posterior shear to capsule strain is likely to be more pronounced. Based on the current results, future quasi-static experiments should control axial rotation rather than axial pretorque to better examine the sensitivity of capsule strain to posterior shear in the presence of an axial rotation.

The quasi-static loading rates used in the current flexibility tests and previously-published failure tests<sup>9</sup> were similar, but nonetheless lower than those present during actual whiplash exposures. Quasi-static loading rates have been shown to affect the magnitude of the load at failure, but maximum principal capsular strain and displacement to failure are not significantly affected by loading rate.<sup>8,20</sup> Thus aside from the unwinding effect described above, the capsular strains reported here are expected to be similar to those present during dynamic whiplash events.

During the multiaxial tests, 2 of 13 specimens (15%) exceeded the strain needed to cause partial failure of the capsule. Although we cannot discount the possibility that other specimens experienced a partial failure during the whiplash-like exposures, the potential for 15% of specimens to exceed a threshold for partial failure is consistent with earlier quasi-static work<sup>8,9</sup> and more recent dynamic work.<sup>21</sup> Similar levels of capsule strains have produced behavioral and electrophysiological evidence of short and long-term pain in animals,<sup>3,4</sup> although both animal experiments strained the dorsal aspect of the capsule rather than the lateral aspect studied here. This 15% risk of partial failure in the capsule is similar to the 12% risk of whiplash-exposed individuals suffering chronic symptoms (>6 months),<sup>22</sup> though considerable work remains to determine whether these similar risk values are related or coincidental.

Two other specimens exceeded the strain needed to cause gross failure of the capsule. There was no evidence of gross failure during our tests and thus this finding likely highlights limitations in our technique. We previously assumed that failures occurred in the element with the highest MPS,<sup>9</sup> yet in this study we compare whiplash and failure strains quadrant-by-quadrant rather than element-by-element. Regional differences in the ligament could also result in different mechanical tolerances at different locations within a quadrant or element.<sup>23</sup> Moreover, the failure tests were conducted along the anteroposterior axis of the facet joint, whereas the whiplash tests exposed the joint to compound three-dimensional displacements. This means that different ligament fibers may have borne the loads during the whiplash and failure tests. Thus even though our tech-

nique provides more detailed strain-field information than other recently-published techniques,<sup>7,21,24</sup> even finer techniques—perhaps looking at region-specific or fiber-specific strains—are needed to capture regional differences and properly characterize the capsular ligament's full three-dimensional behavior during whiplash.<sup>25</sup>

The high strain caused by pretorque alone raises the question of why facet capsular ligaments in these joints are not injured when rotating one's head maximally to the side. Aside from the large rotations taken up at the atlantoaxial joint,<sup>16</sup> one reason may lie in the regional differences described above. The facet capsule likely develops the necessary shape, slack, and tolerance to accommodate voluntary head rotations. The superposition of vertebral retraction during whiplash loading may then shift peak strain to fibers in the capsule that are normally not highly strained during voluntary rotation or combined loading scenarios. Alternatively, the small increase in strain produced by the whiplash loads may be sufficient to injure ligament fibers that are near their limit as a result of a prerotation. Further exploration of this phenomenon will require a more detailed characterization of the dynamic, full-field strains in the facet capsule, and definition of the overall and regional tolerances of the facet capsular ligament and its microstructural components.

In summary, we examined the intervertebral kinematics and facet capsule strains under whiplash-like loads in the presence of an initial axial rotation. We found that an axial rotation doubles the MPS in the capsular ligament compared to the neutral posture. We also found that capsular strains during the simulated whiplash exposure with the head turned were not significantly different from MPS associated with partial failure of the capsule. Thus these findings support the overall hypothesis that excessive capsular strains experienced by some individuals during some whiplash conditions may be responsible for painful capsular whiplash injury.

### ■ Key Points

- Quasi-static loading of cadaveric motion segments was used to examine the effect of a head-turned posture on intervertebral kinematics and facet capsule strain under loading simulating a rear-end collision.
- Compared to a neutral head posture, the maximum principal strain in the facet capsule doubles on the side toward which the head is turned.
- Capsule strains under whiplash-like loading with the head turned are not significantly different from the previously-reported strains needed to cause partial failures in the facet capsule.

### References

1. Dwyer A, Aprill C, Bogduk N. Cervical zygapophyseal joint pain patterns. I: a study in normal volunteers. *Spine* 1990;15:453–7.
2. Lord SM, Barnsley L, Wallis BJ, et al. Chronic cervical zygapophysial joint pain after whiplash. A placebo-controlled prevalence study. *Spine* 1996;21:1737–44.
3. Lu Y, Chen C, Kallakuri S, et al. Neurophysiological and biomechanical characterization of goat cervical facet joint capsules. *J Orthop Res* 2005;23:779–87.
4. Lee KE, Thinnis JH, Gokhin DS, et al. A novel rodent neck pain model of facet-mediated behavioral hypersensitivity: implications for persistent pain and whiplash injury. *J Neurosci Methods* 2004;137:151–9.
5. Sturzenegger M, DiStefano G, Radanov BP, et al. Presenting symptoms and signs after whiplash injury: the influence of accident mechanisms. *Neurology* 1994;44:688–93.
6. Sturzenegger M, Radanov BP, Di Stefano G. The effect of accident mechanisms and initial findings on the long-term course of whiplash injury. *J Neurol* 1995;242:443–9.
7. Panjabi MM, Ivancic PC, Maak TG, et al. Multiplanar cervical spine injury due to head-turned rear impact. *Spine* 2006;31:420–9.
8. Winkelstein BA, Nightingale RW, Richardson WJ, et al. The cervical facet capsule and its role in whiplash injury: a biomechanical investigation. *Spine* 2000;25:1238–46.
9. Siegmund GP, Myers BS, Davis MB, et al. Mechanical evidence of cervical facet capsule injury during whiplash: a cadaveric study using combined shear, compression, and extension loading. *Spine* 2001;26:2095–101.
10. Ono K, Kaneoka K, Wittek A, et al. Cervical injury mechanism based on the analysis of human cervical vertebral motion and head-neck-torso kinematics during low speed rear impact (973340). *Presented at 41st Stapp Car Crash Conference* 1997:339–56.
11. Kaneoka K, Ono K, Inami S, et al. Motion analysis of cervical vertebrae during whiplash loading. *Spine* 1999;24:763–9.
12. Clauser CE, McConville JT, Young JW. Weight, volume, and center of mass of segments of the human body (AMRL-TR-69-70). Yellow Springs, OH: Wright Patterson Air Force Base, Aerospace Medical Research Laboratory; 1969.
13. Siegmund GP, King DJ, Lawrence JM, et al. Head/neck kinematic response of human subjects in low-speed rear-end collisions. *Presented at the 41st Stapp Car Crash Conference* 1997:357–85.
14. Siegmund GP, Brault JR. The role of cervical muscles in whiplash. In: Yoganandan N, Pintar FA, eds. *Frontiers in Whiplash Trauma: Clinical and Biomechanical*. The Netherlands: IOS Press; 2001:295–320.
15. Penning L, Wilmink JT. Rotation of the cervical spine. A CT study in normal subjects. *Spine* 1987;12:732–8.
16. Ishii T, Mukai Y, Hosono N, et al. Kinematics of the subaxial cervical spine in rotation in vivo three-dimensional analysis. *Spine* 2004;29:2826–31.
17. Woltring HJ. Planar control in multi-camera calibration for 3D gait studies. *J Biomech* 1980;13:39–48.
18. Veldpaus FE, Woltring HJ, Dortmans LJMG. A least-squares algorithm for the equiform transformation from spatial marker coordinates. *J Biomech* 1988;21:45–54.
19. Maak TG, Tominaga Y, Panjabi MM, et al. Alar, transverse, and apical ligament strain due to head-turned rear impact. *Spine* 2006;31:632–8.
20. Yoganandan N, Pintar F, Butler J, et al. Dynamic response of human cervical spine ligaments. *Spine* 1989;14:1102–10.
21. Pearson AM, Ivancic PC, Ito S, et al. Facet joint kinematics and injury mechanisms during simulated whiplash. *Spine* 2004;29:390–7.
22. Suissa S, Harder S, Veilleux M. The relation between initial symptoms and signs and the prognosis of whiplash. *Eur Spine J* 2001;10:44–9.
23. Quinn KP, Lee KE, Ahaghotu CC, et al. Structural changes in the cervical facet capsular ligament: potential contributions to pain following subfailure loading. *Stapp Car Crash J* 2007;51:169–87.
24. Stemper BD, Yoganandan N, Pintar FA. Gender- and region-dependent local facet joint kinematics in rear impact: implications in whiplash injury. *Spine* 2004;29:1764–71.
25. Quinn KP, Winkelstein BA. Cervical facet capsular ligament yield defines the threshold for injury and persistent joint mediated neck pain. *J Biomech* 2007;40:299–306.